



Vuolo, L., Stevenson, N. L., Mukhopadhyay, A. G., Roberts, A. J., & Stephens, D. (2020). Cytoplasmic dynein-2 at a glance. *Journal of Cell Science*. <https://doi.org/10.1242/jcs.240614>

Peer reviewed version

Link to published version (if available):  
[10.1242/jcs.240614](https://doi.org/10.1242/jcs.240614)

[Link to publication record in Explore Bristol Research](#)  
PDF-document

This is the author accepted manuscript (AAM). The final published version (version of record) is available online via Company of Biologists at <https://jcs.biologists.org/content/133/6/jcs240614> . Please refer to any applicable terms of use of the publisher.

## University of Bristol - Explore Bristol Research

### General rights

This document is made available in accordance with publisher policies. Please cite only the published version using the reference above. Full terms of use are available:  
<http://www.bristol.ac.uk/red/research-policy/pure/user-guides/ebr-terms/>

# 1 **Cytoplasmic dynein-2 at-a-glance**

2

3 **Laura Vuolo<sup>1</sup>, Nicola L. Stevenson<sup>1</sup>, Aakash G. Mukhopadhyay<sup>2</sup>, Anthony J.**  
4 **Roberts<sup>2</sup>, and David J. Stephens<sup>1\*</sup>**

5 <sup>1</sup> Cell Biology Laboratories, School of Biochemistry, Faculty of Life Sciences, University of  
6 Bristol, BRISTOL, BS8 1TD, UK.

7 <sup>2</sup> Institute of Structural and Molecular Biology, Birkbeck, University of London, London, UK.

8 \*Author for correspondence (david.stephens@bristol.ac.uk)

9

## 10 **ORCID:**

11 **L.V., 0000-0002-9801-9206**

12 **N.L.S., 0000-0001-8967-7277**

13 **A.G.M., 0000-0001-9397-9702**

14 **A.J.R., 0000-0001-5277-6730**

15 **D.J.S., 0000-0001-5297-3240**

16

## 17 **Abstract**

18 Cytoplasmic dynein-2 is a motor protein complex that drives the movement of cargoes  
19 along microtubules within cilia, facilitating the assembly of these organelles on the surface  
20 of nearly all mammalian cells. Dynein-2 is critical for ciliary function as evidenced by  
21 deleterious mutations in patients with skeletal abnormalities. Long-standing questions  
22 include how the dynein-2 complex is assembled, regulated, and switched between active  
23 and inactive states. A combination of model organisms, *in vitro* cell biology, live-cell  
24 imaging, structural biology, and biochemistry has advanced our understanding of the  
25 dynein-2 motor. In this Cell Science at the Glance and the accompanying poster, we  
26 showcase current understanding of dynein-2 and its roles in ciliary assembly and function.

27

28

29 **KEY WORDS: dynein-2, cilia, intraflagellar transport, microtubule motors**

30

## 31 **Introduction**

32 Cytoplasmic dynein-2 (here “dynein-2”) is an ATP-dependent motor protein that steps along  
33 microtubules to transport cargoes within cilia and flagella (Box 1). It is related to  
34 cytoplasmic dynein-1 (here “dynein-1”), which is involved in the transport of cargoes within  
35 the cytoplasm, organelle dynamics (Reck-Peterson et al., 2018), and mitotic spindle  
36 organization during mitosis (Raaijmakers and Medema, 2014). In contrast, dynein-2 does  
37 not act in canonical membrane traffic (Palmer et al., 2009), but functions primarily, if not  
38 exclusively, within the intraflagellar transport (IFT) system (Box 2). Here, dynein-2  
39 assembles with kinesin-2, IFT-A complexes, and IFT-B complexes to form polymeric IFT  
40 “trains”, which move cargoes to the ciliary tip (kinesin-2 direction) and back to the cell body  
41 (dynein-2 direction). Dynein-2-driven transport occurs in the confined space between the  
42 ciliary microtubule doublets and the ciliary membrane (Roberts, 2018). There is some  
43 evidence for dynein-2 functions outside of cilia; for example, in *Chlamydomonas*, which  
44 lacks dynein-1, dynein-2 is implicated in cytoplasmic trafficking to the base of cilia (Cao et  
45 al., 2015).

46 Dynein-1 and dynein-2 are distantly related to their axonemal cousins (Kollmar, 2016;  
47 Wickstead and Gull, 2007), which drive the beating of motile cilia and flagella (Box 1).  
48 Below, and in the accompanying poster, we provide an overview of dynein-2 discovery,  
49 subunit composition, structure, and regulation. We also discuss new insights into the  
50 functions of dynein-2 in maintaining the ciliary transition zone – the gatekeeper between  
51 the cilium and the cytoplasm (Box 1) – as well as the connection between dynein-2 and  
52 human disease.

## 53 **Discovery of dynein-2 and its role in IFT**

54 Dynein-2 was first identified in sea-urchin (Gibbons et al., 1994) and rat (Tanaka et al.,  
55 1995) based on sequence similarity to dynein-1 in mammals. It was described as a  
56 cytoplasmic dynein and shown to be upregulated prior to ciliogenesis in sea urchin  
57 embryos (Gibbons et al., 1994) and mammalian cells (Criswell et al., 1996). Retrograde  
58 IFT was first linked to a cytoplasmic dynein motor in *Chlamydomonas* (Pazour et al.,  
59 1998). Further work revealed that mutations in dynein-2 resulted in cells with short flagella  
60 that accumulated IFT proteins at their tip (Pazour et al., 1999b; Pazour et al., 1998; Porter  
61 et al., 1999), and also perturbed retrograde transport of kinesin-2 in *C. elegans* (Signor et  
62 al., 1999).

## 63 **Structure and composition of dynein-2**

64 Dynein-2 is a large multiprotein complex, composed of 16 copies of at least eight different  
65 proteins in humans (see poster). Insights into dynein-2 subunit composition have come  
66 from a variety of cell biology, genetic, and biochemical studies (see below), and a recent  
67 cryo-EM structure of the dynein-2 complex (Toropova et al., 2019). Like other dyneins, the  
68 subunits of dynein-2 are classified as heavy chains, intermediate chains, light-intermediate  
69 chains, and light chains depending on their mass. Most subunits in the dynein-2 complex  
70 are unique to dynein-2, but a subset of the light chains are also found in dynein-1 (Asante  
71 et al., 2014). Naming of dynein-2 subunits varies (see poster) and here we use the human  
72 nomenclature unless specified.

73 Dynein-2 is built around two copies of the heavy chain, DYNC2H1 (Criswell et al., 1996;  
74 Mikami et al., 2002). The C-terminal region forms the motor domain, which converts the  
75 energy from ATP hydrolysis into movement (Schmidt et al. 2015). The N-terminal region  
76 forms the tail: an extended structure that binds the other subunits (Hamada et al., 2018)  
77 and holds the two heavy chains in a homodimer (Toropova et al., 2017; Toropova et al.,  
78 2019). In an interesting variation compared to other organisms, trypanosomatids possess  
79 two distinct dynein-2 heavy chains that form a heterodimer (Adhiambo et al., 2005; Blisnick  
80 et al., 2014).

81 The dynein-2 light-intermediate chain, DYNC2LI1 (Grissom et al., 2002; Hao et al., 2011;  
82 Hou et al., 2004; Li et al., 2015; Mikami et al., 2002), binds directly to the tail of each heavy  
83 chain and is important for stabilising its structure (Hou et al., 2004; Reck et al., 2016;  
84 Toropova et al., 2017). The light-intermediate chain has a Ras-like fold and appears to  
85 bind to nucleotide (Schroeder et al., 2014; Toropova et al., 2019). Although nucleotide-  
86 binding by the light-intermediate chain does not seem essential for dynein-2 function (Hou  
87 et al., 2004), whether it serves a structural role or has a minor regulatory function remains  
88 unclear.

89 The other dynein-2 subunits – namely, the intermediate chains and light chains – form an  
90 unusual stoichiometry subcomplex at the core of dynein-2's tail, which makes the structure  
91 of dynein-2 highly asymmetric (Toropova et al., 2019). While dynein-1 is composed of  
92 homodimeric subunits, including its intermediate chain, dynein-2 notably differs in that it  
93 contains two different intermediate chains. Originally defined as FAP133 (Rompolas et al.,  
94 2007) and FAP163 (Patel-King et al., 2013) in *Chlamydomonas*, these subunits have been  
95 validated as *bona fide* mammalian dynein-2 subunits, WDR34 (Asante et al., 2013; Asante

96 et al., 2014; Huber et al., 2013; Schmidts et al., 2013b) and WDR60 (Asante et al., 2014;  
97 McInerney-Leo et al., 2013).

98 WDR34 and WDR60 form a heterodimer (Asante et al., 2014; Hamada et al., 2018;  
99 Toropova et al., 2019; Vuolo et al., 2018) (see poster). Their C-terminal  $\beta$ -propeller  
100 domains each bind a copy of the heavy chain, and their extended N-terminal regions are  
101 held together by an array of light chain dimers (Toropova et al., 2019). These comprise  
102 one DYNLRB dimer, which binds proximal to the  $\beta$ -propellers, followed by three DYNLL  
103 dimers, and a putative DYNLT-TCTEX1D2 heterodimer (Asante et al., 2014; Hamada et  
104 al., 2018; Kanie et al., 2017; Toropova et al., 2019; Tsurumi et al., 2019). Co-expression  
105 studies indicate that WDR34 preferentially interacts with DYNLL and DYNLRB, whereas  
106 WDR60 preferentially interacts with DYNLT-TCTEX1D2 (Hamada et al., 2018). Among the  
107 light chains, TCTEX1D2 is specific to dynein-2 (Asante et al., 2014; Gholkar et al., 2015;  
108 Schmidts et al., 2015). The other light chains (DYNLRB, DYNLL, and DYNLT) are also  
109 found in dynein-1 (Asante et al., 2014), and each has two orthologs in mammals (e.g.  
110 DYNLRB1 and DYNLRB2). The orthologs appear to play interchangeable roles (Hamada  
111 et al., 2018) but may have subtly different biochemical properties or generate tissue-  
112 specific expression patterns (King et al., 1998). In summary, the unusual stoichiometry of  
113 dynein-2's intermediate and light chains is a distinctive feature of the complex; as  
114 described below, it has important roles in dynein-2 motility regulation and attachment to  
115 IFT trains.

## 116 **Regulation and Motility**

117 Dynein-2 motility is tightly regulated to enable its functions in IFT. The dynein-2 motor  
118 domain contains a ring of six AAA+ modules, of which the N-proximal module (AAA1) is  
119 the main ATPase site (Schmidt et al., 2015). N-terminal to AAA1 is a rod-like 'linker'  
120 domain that amplifies conformational changes. Dynein-2's microtubule-binding domain is  
121 at the tip of a coiled-coil stalk (see poster).

122 The current generally accepted model is that dynein-2 is transported passively from the  
123 ciliary base to tip by kinesin-2 (Hao et al., 2011; Rosenbaum and Witman, 2002).

124 Following activation, it then actively transports the IFT machinery and cargoes from tip to  
125 base during retrograde IFT. The motile properties of the human dynein-2 motor domain  
126 have been recently described using *in vitro* assays (Toropova et al., 2017). Interestingly,  
127 monomeric constructs moved significantly faster (around 500 nm/s) than dimers, as the  
128 motor domains in the dimer stack against one another to give rise to an auto-inhibited

129 conformation (Toropova et al., 2017; Toropova et al., 2019). Accordingly, disruption of the  
130 stacking interface induced a significant increase in velocity. These results suggested that  
131 the dynein-2 motor domains intrinsically exist in an autoinhibited, stacked conformation,  
132 that facilitates transport of dynein-2 to the ciliary tip by kinesin-2 (Toropova et al., 2017).  
133 Supporting this model, motility assays using both kinesin-2 and dynein-2 showed that the  
134 velocity of kinesin-2 was only minimally affected by inactive dynein-2, whereas an  
135 unstacked, active dynein-2 mutant conferred resistance against kinesin-2 (Toropova et al.,  
136 2017). *In vivo* support for dynein-2 auto-inhibition came from an analysis of IFT trains by  
137 using cryo-electron tomography in *Chlamydomonas* (Jordan et al., 2018). In this study, the  
138 anterograde trains were observed as densely packed and ordered structures composed of  
139 three repeats of approximately of 6, 11 and 18 nm, which were assigned to IFT-B, IFT-A  
140 and dynein-2 respectively. Notably, dynein-2 appeared in a stacked (autoinhibited)  
141 conformation when interacting with anterograde trains, with its stalks oriented away from  
142 the microtubule, which is likely to further inhibit the motor.

143 Recent cryo-EM and cryo-electron tomography studies shed light on how dynein-2's  
144 subunits enable it to associate with anterograde IFT trains to travel to the ciliary tip. In  
145 particular, dynein-2's subcomplex of intermediate and light chains has at least two  
146 important roles. First, it brings two copies of the heavy chain together into a stable dimer  
147 with auto-inhibited motors domains (Toropova et al., 2019), which is likely a suitable state  
148 for loading onto anterograde trains at the ciliary base (Wingfield et al., 2017). Second, the  
149 intermediate and light chains contort the two copies of the heavy chain into different  
150 conformations within the tail (Toropova et al., 2019). This asymmetric architecture is  
151 tailored to the repeating structure of the anterograde IFT-B train: each dynein-2 complex  
152 spreads out over seven to eight IFT-B repeats, and is tightly packed with the neighbouring  
153 dynein-2 complexes along the train (Jordan et al., 2018; Toropova et al., 2019) An  
154 important question for future studies is to determine which subunits of the IFT-B complex  
155 interact with dynein-2 on the anterograde train, but molecular genetic studies have  
156 implicated IFT172 as important for dynein-2 targeting or turnaround the ciliary tip  
157 (Pedersen et al., 2005; Tsao and Gorovsky, 2008; Williamson et al., 2012).

158 The mechanism by which dynein-2 is repositioned to bind to the axoneme and switched to  
159 an active conformation at the tip remains one of the most intriguing questions in the field.  
160 Biochemical and genetic studies suggest that classical dynein-1 accessory factors such as  
161 dynactin (Reck-Peterson et al., 2018) are not involved in dynein-2 regulation (Asante et al.,  
162 2014; Roberts, 2018). One possibility is that IFT-A and IFT-B themselves regulate dynein-

163 2 activity and that the rearrangement of these large complexes during train disassembly  
164 and reassembly facilitates a conformational switch within dynein-2 to form an active  
165 complex at the ciliary tip (Yi et al., 2017). Because the intermediate and light chains  
166 stabilise the auto-inhibited conformation of dynein-2, they must either rearrange or  
167 dissociate to activate the motor at the ciliary tip (Pazour et al., 2000; Toropova et al.,  
168 2019). Post-translational modifications of dynein-2 of the IFT subunits might have a role in  
169 dynein-2 activation, but these are not yet well described. It is also possible that other, thus  
170 far unknown regulators, are involved in this process.

### 171 **Ciliogenesis and cilia function in dynein-2 mutants**

172 Mutants in the dynein-2 heavy chain in many model organisms, including  
173 *Chlamydomonas*, *C. elegans*, mouse and zebrafish, and cultured mammalian cells,  
174 present similar phenotypes with short cilia and bulbous ciliary tips (Adhiambo et al., 2005;  
175 May et al., 2005; Pazour et al., 1999a; Porter et al., 1999; Wicks et al., 2000). In both mice  
176 (Wu et al., 2017) and cultured human cells (Vuolo et al., 2018), loss of WDR34 is  
177 associated with severe ciliogenesis defects, but others have shown that ciliogenesis is  
178 only moderately impaired in WDR34 knock-out (KO) cells (Tsurumi et al., 2019). In  
179 contrast, WDR60 is required for correct retrograde trafficking, but is dispensable for  
180 extending the ciliary axoneme in cultured human cells (Asante et al., 2014; Hamada et al.,  
181 2018; Vuolo et al., 2018). Moreover, fibroblasts from affected individuals with mutations in  
182 WDR60 still extend the ciliary axoneme, but the percentage of ciliated cells is variable  
183 (McInerney-Leo et al., 2013). Similar phenotypes with normal cilia length and a moderate  
184 reduction in cilia number were observed in TCTEX1D2 mutant fibroblasts from affected  
185 individual with short rib–polydactyly syndromes (SRPS) (Schmidts et al., 2015) or in  
186 TCTEX1D2-KO cells (Hamada et al., 2018).

187 Although defects in DYNC2LI1 do not completely abolish cilia extension, its mutation is  
188 associated with a ciliary accumulation of IFT proteins and defects in cilia length regulation,  
189 as observed in patient fibroblasts (Kessler et al., 2015; Taylor et al., 2015). Moreover,  
190 DYNC2LI1 appears to play a critical role in the stability of the dynein-2 complex in  
191 *Chlamydomonas* (Hou et al., 2004; Reck et al., 2016). These variations in phenotype could  
192 result from low level expression or, in some cases of genome engineering, expression of  
193 truncated proteins, leading to retention of partial function. Furthermore, loss of one subunit  
194 may affect the overall stability of the complex as has been seen for WDR34 and WDR60  
195 KO. This outcome has also been clearly described for mice lacking the transcription factor  
196 ASCIZ (ATMIN) which have a severely reduced expression of the LC8 light chain,

197 DYNLL1, which results in partial depletion other dynein-2 subunits (King et al., 2019).  
198 Overall, full dynein-2 function does not appear to be absolutely required for ciliogenesis  
199 *per se*, but is needed to maintain the overall structure, including length control, and for  
200 core ciliary signalling functions.

### 201 **Dynein-2 and the ciliary transition zone**

202 New insights into IFT trafficking recently revealed an unexpected role for IFT-A and  
203 dynein-2 in maintaining compartmentalization of the transition zone (TZ) and thus of the  
204 ciliary structure in *C. elegans* and human cells. The TZ consist of a densely packed  
205 domain containing multiple proteins that are assembled in a tightly regulated process (see  
206 Box 1 and poster). The hierarchy of TZ assembly has been extensively described in  
207 several organisms and presents some common features in different models (reviewed in  
208 (Goncalves and Pelletier, 2017)). Super-resolution imaging and electron microscopy have  
209 resolved a map that defines the localization of distinct modules of the TZ (see poster).  
210 CEP290 (centrosomal protein 290 kDa) lies at the core of the TZ base and facilitates the  
211 assembly of other TZ components (Yang et al., 2015). RPGRIP1L ((retinitis pigmentosa  
212 GTPase regulator interacting protein 1-like; also called MKS-5 (Meckel syndrome type 5))  
213 is a core component of *C. elegans* and vertebrate TZs (Li et al., 2016; Wiegering et al.,  
214 2018) that localizes distally to CEP290 and adjacent to the TZ microtubules. The NPHP  
215 (nephronophthisis) module links the CEP290 core to the MKS module that includes MKS1  
216 (Meckel syndrome type 1), TCTN1 (Tectonic-1), TCTN2 (Tectonic-2), as well as several  
217 membrane proteins including TMEM67 (transmembrane protein 67) (Awata et al., 2014;  
218 Dean et al., 2016; Goncalves and Pelletier, 2017; Schouteden et al., 2015; Wang et al.,  
219 2013). This organization is also supported by proteomic mapping of the base of the cilium  
220 (Gupta et al., 2015). The TZ links the axonemal microtubules to the ciliary membrane and  
221 acts to gate entry and exit of proteins and lipids to the cilium. As such, it serves a vital  
222 function in the compartmentalization of ciliary signalling.

223 Recent data showed that dynein-2 is important to maintain the structure and integrity of the  
224 TZ. Loss of dynein-2 intermediate chains WDR34 and WDR60 caused a disruption of TZ  
225 composition in cultured human cells (Jensen et al., 2018; Vuolo et al., 2018), and a  
226 temperature-sensitive mutant showed that dynein-2 is required for TZ assembly and gating  
227 function in *C. elegans* (Jensen et al., 2018). In particular, the studies in human cells  
228 showed a distal extension of the RPGRIP1L domain of the TZ and a reduction of the  
229 TMEM67 area, whereas other TZ components, such as TCTN1 and CEP290, were not



230 affected. Interestingly, knockout of WDR34 and WDR60 was also associated with  
231 mislocalisation of several ciliary membrane proteins and IFT components, suggesting a  
232 defect in the entry and/or export mechanism that is regulated by the TZ (Vuolo et al.,  
233 2018). Consistent with these data, the temperature-sensitive mutation in the dynein-2  
234 heavy chain resulted in a defective TZ composition in *C. elegans* (Jensen et al., 2018).  
235 Notably, at the restrictive temperature, some TZ components, such as NPHP4  
236 (nephrocystin 4), CEP290 and MKS6 (Meckel Syndrome, Type 6), were mislocalised to a  
237 more distal region of the cilium. Furthermore, disruption of the TZ resulted in the ectopic  
238 localization of two different basal body proteins, TRAM1 (Translocating Chain-Associating  
239 Membrane Protein) and RPI2 (human retinitis pigmentosa-2 ortholog), in the ciliary  
240 axoneme (Jensen et al., 2018), suggesting a defect in the 'ciliary gate' formed by the TZ.  
241 Interestingly, proper TZ organisation was restored at permissive temperature, indicating  
242 that maintenance of TZ integrity is an active process that requires dynein-2.

243 It is uncertain how dynein-2 mediates TZ assembly, but this might involve its association  
244 with the IFT-A complex (Scheidel and Blacque, 2018). Analysis of IFT-A mutants indicated  
245 that IFT-A components play different roles in cilia entry and/or export of TZ components in  
246 the cilia in *C. elegans*. According to this model, core subunits of IFT-A (e.g. IFT140)  
247 promote entry of TZ proteins into cilia, whereas its non-core subunits (IFT121, IFT139,  
248 IFT43) regulate ciliary export. Consistent with observations in dynein-2 KO-cells (Vuolo et  
249 al., 2018), the key TZ component RPGRIP1 is mislocalised in IFT-A mutants. Although  
250 the cilia from both IFT-A and dynein-2 mutants show a mislocalisation of several TZ  
251 proteins, no major defects are observed in the overall architecture of the TZ as determined  
252 by electron microscopy (Jensen et al., 2018). High-resolution views of the structure and  
253 dynamics of the TZ's components may help to elucidate its gating function and  
254 dependence on IFT-A and dynein-2.

### 255 **Human diseases associated with defects in dynein-2 function**

256 Defects in cilia formation and function lead to human pathologies, collectively termed  
257 ciliopathies (Reiter and Leroux, 2017). Mutations in dynein-2 are associated with a group  
258 of ciliopathies called 'skeletal ciliopathies' that are described as dysplasia (SRTD) with or  
259 without polydactyly (Huber and Cormier-Daire, 2012). The phenotypes related to skeletal  
260 ciliopathies include craniofacial abnormalities, short stature, shortened ribs, brachydactyly,  
261 and polydactyly. The skeletal phenotype can appear in association with defects in other  
262 organs, with retinal and kidney abnormalities as the most common symptoms observed

263 outside the skeletal system (Huber and Cormier-Daire, 2012). The skeletal abnormalities  
264 observed in some forms of SRTD patients are most likely related to defects in signalling  
265 pathways during embryonic development, including hedgehog (Hh), which requires cilia  
266 (Huangfu et al., 2003). In this context, cilia are particularly important to ensure correct Hh  
267 signalling during bone formation, and defects in dynein-2 result in the mislocalisation of  
268 Smoothed, a key component of Hh signalling, to cilia (May et al., 2005; Tsurumi et al.,  
269 2019; Vuolo et al., 2018; Wu et al., 2017). In recent years, whole exome-sequencing has  
270 enabled the identification of new mutations involved in skeletal ciliopathies, with the most  
271 common mutations affecting DYNC2H1 (Badiner et al., 2017; Cossu et al., 2016;  
272 Dagoneau et al., 2009; Merrill et al., 2009; Schmidts et al., 2013a). Moreover, mutations in  
273 WDR34 (Huber et al., 2013; Schmidts et al., 2013b), WDR60 (Cossu et al., 2016;  
274 McInerney-Leo et al., 2013), DYNC2LI1 (Kessler et al., 2015; Taylor et al., 2015), and  
275 TCTEX1D2 (Gholkar et al., 2015; Schmidts et al., 2015) have been also associated with  
276 SRTD, and a conditional KO of DYNLL1 in mouse limb mesoderm resulted in bone  
277 shortening, similar to that observed in SRTD patients (King et al., 2019). A comprehensive  
278 review of dynein-2 genes associated with skeletal ciliopathies has been recently published  
279 (Schmidts and Mitchison, 2018).

## 280 **Conclusions**

281 While we know much about the composition of the dynein-2 motor, its interactions, and  
282 now even have a structure of the dynein-2 complex, there is still much to be determined. A  
283 question for both mechanistic and clinical studies is how defects in dynein-2 relate to  
284 anterograde and retrograde trafficking. The tight co-assembly of dynein-2 with IFT-B trains  
285 defines its crucial position in anterograde IFT trains (Jordan et al., 2018; Toropova et al.,  
286 2019). Understanding the role of dynein-2 in maintaining a functional cilium and  
287 coordinating different signalling pathways, notably Hh, will likely help us to understand the  
288 contributions of dynein-2 and cilia in and skeletogenesis. Open questions include how, at  
289 the atomic level, dynein-2 co-assembles with IFT complexes at the ciliary base, and how  
290 its entry into the cilium is gated. It is also unclear what triggers the disassembly of  
291 anterograde kinesin-2-driven IFT trains at the ciliary tip, how retrograde trains - driven by  
292 active dynein-2 - are formed, or why dynein-2 is used to actively transport kinesin-2 to the  
293 ciliary base in vertebrate cilia (Broekhuis et al., 2014; Williams et al., 2014) when diffusion  
294 appears to be sufficient in *Chlamydomonas* (Chien et al., 2017; Engel et al., 2012).

295 Intensive and integrated efforts combining biochemistry, structural biology, clinical  
296 genetics, cell and developmental biology will be required to address these challenges,  
297 giving an opportunity to fully understand the mechanism and functions of dynein-2 in cilia  
298 biology and to apply this knowledge to improve human health.

### 299 **Competing interests**

300 The authors declare no competing or financial interests.

301

### 302 **Funding**

303 L.V., A.G.M., A.J.R. and D.J.S. work on dynein-2 is funded by a collaborative grant from  
304 UK Research and Innovation-Biotechnology and Biological Sciences Research Council  
305 (UKRI-BBSRC, BB/S005390/1). Further work in D.J.S.'s laboratory on dynein-2 is  
306 supported by UKRI-BBSRC [BB/S013024/1] and in A.J.R.'s laboratory by UKRI-BBSRC  
307 [BB/S007202/1 and BB/P008348/1] and The Wellcome Trust and Royal Society  
308 [104196/Z/14/Z].

309

310

311 **BOX 1: Primary and motile cilia**

312 Cilia are microtubule-based structures, with an axoneme based on nine cylindrically  
313 arranged microtubule (MT) doublets. Primary (a.k.a. sensory) cilia are solitary structures  
314 on the cell surface and function as 'antenna' that transduce signals from the extracellular  
315 environment. Motile cilia are present on specialised cell types and function to drive the  
316 movement of fluids in multiciliated epithelia in vertebrates, the locomotion of sperm, and  
317 the motility of many unicellular organisms. In addition to the nine microtubules doublets,  
318 motile cilia usually feature an additional central pair of MTs in the axoneme lumen (Mirvis  
319 et al., 2018). Axonemal dyneins generate the force to bend the axoneme in motile cilia  
320 (King and Sale, 2018). In all cilia and flagella, each microtubule doublet consists of A and  
321 B tubules, with the A tubule formed by 13 protofilaments and the B tubule formed by 10  
322 protofilaments. While motile cilia typically present a 9+2 structure along the axoneme  
323 length, the structure of primary cilia is more variable. Recent electron tomography data  
324 indicate that in the primary cilium of several kidney cell lines, two of the microtubule  
325 doublets progressively shift toward the core of the axoneme at the region where the  
326 primary cilium starts to extend into the extracellular space, forming a 7+2 arrangement  
327 (Sun et al., 2019).

328 The structure of cilia includes a series of evolutionarily conserved subdomains, each  
329 defined by a specific cohort of proteins. The cilium extends from the basal body, formed by  
330 the mother centriole along with subdistal and distal appendages proteins. Transition fibres  
331 connect the basal body to the plasma membrane. Distal to the basal body is the transition  
332 zone (TZ), characterized by membrane-associated Y-shaped links. Transition fibres and  
333 the TZ compartment form a permeability barrier called the 'ciliary gate' that regulate ciliary  
334 protein composition (Jensen and Leroux, 2017) (see poster) .

335

## 336 **BOX 2: The bidirectional intraflagellar transport system**

337 IFT was first described in *Chlamydomonas reinhardtii*, where large particles moving in both  
338 directions along the length of the flagella were observed using differential interference  
339 contrast (DIC) microscopy (Kozminski et al., 1993). Subsequently, using time-lapse  
340 imaging of specifically-labelled proteins, IFT has been described in many model systems,  
341 including *Caenorhabditis elegans* (Orozco et al., 1999), *Tetrahymena thermophila* (Brown  
342 et al., 1999), *Trypanosoma brucei* (Absalon et al., 2008) and vertebrate cells (Follit et al.,  
343 2006; Pazour et al., 2002; Pazour et al., 2000). IFT trafficking complexes called 'trains'  
344 comprise IFT-A and IFT-B subcomplexes, which mediate the interactions between the  
345 ciliary motors and cargo (see poster). The IFT-B complex is generally associated with  
346 anterograde trafficking; it is formed of a core subcomplex of 10 subunits (IFT88, -81, -74, -  
347 70, --56, 52, -46, -27, -25, and -22), a peripheral complex of six subunits (IFT172, -80, -57,  
348 -54, -38, and -20), and associates with the small GTPase RabL2 (Kanie et al., 2017). IFT-  
349 A, which is generally required for retrograde transport as well as the ciliary import of a  
350 variety of membrane proteins, includes IFT144, -140, -139, -122, -121, and -43 (Taschner  
351 and Lorentzen, 2016), and associates with the cargo adapter TULP3 (Mukhopadhyay  
352 2010). A further complex, the BBSome, associates with IFT trains to stabilise their  
353 assembly (Wei et al., 2012) and mediates retrograde membrane protein trafficking  
354 (Nachury and Mick, 2019). In *Chlamydomonas*, anterograde and retrograde IFT trains  
355 have been defined to move on the B and A tubules of the axonemal microtubule doublets,  
356 respectively (Stepanek and Pigino, 2016). While there are strong common features of IFT  
357 between model organisms, there are also key differences. In *Chlamydomonas*, kinesin-2  
358 appears to mainly diffuse back to the ciliary base (Engel et al., 2012), whereas, in  
359 metazoans, kinesin-2 motors appear to be recycled to the ciliary base predominantly by  
360 retrograde IFT (Mijalkovic et al., 2017; Signor et al., 1999; Vuolo et al., 2018; Williams et  
361 al., 2014). Interestingly, an additional dynein heavy chain, DHC-3, has been implicated in  
362 the formation of a subset of cilia in *C. elegans*, and DHC-3 was identified – together with  
363 the dynein-2 heavy chain - in genetic screens for anti-helminth resistance (Page, 2018).  
364 The deposited protein sequence for DHC-3 suggests it is a highly divergent dynein heavy  
365 chain that lacks ATP binding sites that is thus unlikely to function as a conventional motor.

366

367 **References**

- 368 **Absalon, S., Blisnick, T., Kohl, L., Toutirais, G., Dore, G., Julkowska, D., Tavenet, A. and Bastin, P.**  
369 (2008). Intraflagellar transport and functional analysis of genes required for flagellum formation in  
370 trypanosomes. *Mol Biol Cell* **19**, 929-44.
- 371 **Adhiambo, C., Forney, J. D., Asai, D. J. and LeBowitz, J. H.** (2005). The two cytoplasmic dynein-2  
372 isoforms in *Leishmania mexicana* perform separate functions. *Mol Biochem Parasitol* **143**, 216-25.
- 373 **Asante, D., Maccarthy-Morrogh, L., Townley, A. K., Weiss, M. A., Katayama, K., Palmer, K. J.,**  
374 **Suzuki, H., Westlake, C. J. and Stephens, D. J.** (2013). A role for the Golgi matrix protein giantin in  
375 ciliogenesis through control of the localization of dynein-2. *Journal of Cell Science* **126**, 5189-97.
- 376 **Asante, D., Stevenson, N. L. and Stephens, D. J.** (2014). Subunit composition of the human  
377 cytoplasmic dynein-2 complex. *Journal of Cell Science* **127**, 4774-87.
- 378 **Awata, J., Takada, S., Standley, C., Lechtreck, K. F., Bellevue, K. D., Pazour, G. J., Fogarty, K. E. and**  
379 **Witman, G. B.** (2014). NPHP4 controls ciliary trafficking of membrane proteins and large soluble proteins at  
380 the transition zone. *Journal of Cell Science* **127**, 4714-27.
- 381 **Badiner, N., Taylor, S. P., Forlenza, K., Lachman, R. S., University of Washington Center for**  
382 **Mendelian, G., Bamshad, M., Nickerson, D., Cohn, D. H. and Krakow, D.** (2017). Mutations in *DYNC2H1*,  
383 the cytoplasmic dynein 2, heavy chain 1 motor protein gene, cause short-rib polydactyly type I, Saldino-  
384 Noonan type. *Clin Genet* **92**, 158-165.
- 385 **Blisnick, T., Buisson, J., Absalon, S., Marie, A., Cayet, N. and Bastin, P.** (2014). The intraflagellar  
386 transport dynein complex of trypanosomes is made of a heterodimer of dynein heavy chains and of light  
387 and intermediate chains of distinct functions. *Mol Biol Cell* **25**, 2620-33.
- 388 **Broekhuis, J. R., Verhey, K. J. and Jansen, G.** (2014). Regulation of cilium length and intraflagellar  
389 transport by the RCK-kinases ICK and MOK in renal epithelial cells. *PLoS One* **9**, e108470.
- 390 **Brown, J. M., Marsala, C., Kosoy, R. and Gaertig, J.** (1999). Kinesin-II is preferentially targeted to  
391 assembling cilia and is required for ciliogenesis and normal cytokinesis in *Tetrahymena*. *Mol Biol Cell* **10**,  
392 3081-96.
- 393 **Cao, M., Ning, J., Hernandez-Lara, C. I., Belzile, O., Wang, Q., Dutcher, S. K., Liu, Y. and Snell, W. J.**  
394 (2015). Uni-directional ciliary membrane protein trafficking by a cytoplasmic retrograde IFT motor and  
395 ciliary ectosome shedding. *Elife* **4**.
- 396 **Chien, A., Shih, S. M., Bower, R., Tritschler, D., Porter, M. E. and Yildiz, A.** (2017). Dynamics of the  
397 IFT machinery at the ciliary tip. *Elife* **6**.
- 398 **Cossu, C., Incani, F., Serra, M. L., Coiana, A., Crisponi, G., Boccone, L. and Rosatelli, M. C.** (2016).  
399 New mutations in *DYNC2H1* and *WDR60* genes revealed by whole-exome sequencing in two unrelated  
400 Sardinian families with Jeune asphyxiating thoracic dystrophy. *Clin Chim Acta* **455**, 172-80.
- 401 **Criswell, P. S., Ostrowski, L. E. and Asai, D. J.** (1996). A novel cytoplasmic dynein heavy chain:  
402 expression of *DHC1b* in mammalian ciliated epithelial cells. *Journal of Cell Science* **109 ( Pt 7)**, 1891-8.
- 403 **Dagoneau, N., Goulet, M., Genevieve, D., Sznajder, Y., Martinovic, J., Smithson, S., Huber, C.,**  
404 **Baujat, G., Flori, E., Tecco, L. et al.** (2009). *DYNC2H1* mutations cause asphyxiating thoracic dystrophy and  
405 short rib-polydactyly syndrome, type III. *American Journal of Human Genetics* **84**, 706-11.
- 406 **Dean, S., Moreira-Leite, F., Varga, V. and Gull, K.** (2016). Cilium transition zone proteome reveals  
407 compartmentalization and differential dynamics of ciliopathy complexes. *Proc Natl Acad Sci U S A* **113**,  
408 E5135-43.
- 409 **Engel, B. D., Ishikawa, H., Wemmer, K. A., Geimer, S., Wakabayashi, K., Hirono, M., Craige, B.,**  
410 **Pazour, G. J., Witman, G. B., Kamiya, R. et al.** (2012). The role of retrograde intraflagellar transport in  
411 flagellar assembly, maintenance, and function. *J Cell Biol* **199**, 151-67.
- 412 **Follit, J. A., Tuft, R. A., Fogarty, K. E. and Pazour, G. J.** (2006). The intraflagellar transport protein  
413 IFT20 is associated with the Golgi complex and is required for cilia assembly. *Mol Biol Cell* **17**, 3781-92.
- 414 **Gholkar, A. A., Senese, S., Lo, Y. C., Capri, J., Deardorff, W. J., Dharmarajan, H., Contreras, E.,**  
415 **Hodara, E., Whitelegge, J. P., Jackson, P. K. et al.** (2015). *Tctex1d2* associates with short-rib polydactyly  
416 syndrome proteins and is required for ciliogenesis. *Cell Cycle* **14**, 1116-25.
- 417 **Gibbons, B. H., Asai, D. J., Tang, W. J., Hays, T. S. and Gibbons, I. R.** (1994). Phylogeny and  
418 expression of axonemal and cytoplasmic dynein genes in sea urchins. *Molecular Biology of the Cell* **5**, 57-70.

419 **Goncalves, J. and Pelletier, L.** (2017). The Ciliary Transition Zone: Finding the Pieces and  
420 Assembling the Gate. *Mol Cells* **40**, 243-253.

421 **Grissom, P. M., Vaisberg, E. A. and McIntosh, J. R.** (2002). Identification of a novel light  
422 intermediate chain (D2LIC) for mammalian cytoplasmic dynein 2. *Molecular Biology of the Cell* **13**, 817-29.

423 **Gupta, G. D., Coyaud, E., Goncalves, J., Mojarad, B. A., Liu, Y., Wu, Q., Gheiratmand, L., Comartin,  
424 D., Tkach, J. M., Cheung, S. W. et al.** (2015). A Dynamic Protein Interaction Landscape of the Human  
425 Centrosome-Cilium Interface. *Cell* **163**, 1484-99.

426 **Hamada, Y., Tsurumi, Y., Nozaki, S., Katoh, Y. and Nakayama, K.** (2018). Interaction of WDR60  
427 intermediate chain with TCTEX1D2 light chain of the dynein-2 complex is crucial for ciliary protein  
428 trafficking. *Mol Biol Cell* **29**, 1628-1639.

429 **Hao, L., Efimenko, E., Swoboda, P. and Scholey, J. M.** (2011). The retrograde IFT machinery of *C.*  
430 *elegans* cilia: two IFT dynein complexes? *PLoS One* **6**, e20995.

431 **Hou, Y., Pazour, G. J. and Witman, G. B.** (2004). A dynein light intermediate chain, D1bLIC, is  
432 required for retrograde intraflagellar transport. *Mol Biol Cell* **15**, 4382-94.

433 **Huangfu, D., Liu, A., Rakeman, A. S., Murcia, N. S., Niswander, L. and Anderson, K. V.** (2003).  
434 Hedgehog signalling in the mouse requires intraflagellar transport proteins. *Nature* **426**, 83-7.

435 **Huber, C. and Cormier-Daire, V.** (2012). Ciliary disorder of the skeleton. *Am J Med Genet C Semin  
436 Med Genet* **160C**, 165-74.

437 **Huber, C., Wu, S., Kim, A. S., Sigaudy, S., Sarukhanov, A., Serre, V., Baujat, G., Le Quan Sang, K. H.,  
438 Rimoin, D. L., Cohn, D. H. et al.** (2013). WDR34 Mutations that Cause Short-Rib Polydactyly Syndrome Type  
439 III/Severe Asphyxiating Thoracic Dysplasia Reveal a Role for the NF-kappaB Pathway in Cilia. *American  
440 Journal of Human Genetics* **93**, 926-31.

441 **Jensen, V. L., Lambacher, N. J., Li, C., Mohan, S., Williams, C. L., Inglis, P. N., Yoder, B. K., Blacque,  
442 O. E. and Leroux, M. R.** (2018). Role for intraflagellar transport in building a functional transition zone.  
443 *EMBO Rep* **19**.

444 **Jensen, V. L. and Leroux, M. R.** (2017). Gates for soluble and membrane proteins, and two  
445 trafficking systems (IFT and LIFT), establish a dynamic ciliary signaling compartment. *Curr Opin Cell Biol* **47**,  
446 83-91.

447 **Jordan, M. A., Diener, D. R., Stepanek, L. and Pigino, G.** (2018). The cryo-EM structure of  
448 intraflagellar transport trains reveals how dynein is inactivated to ensure unidirectional anterograde  
449 movement in cilia. *Nat Cell Biol* **20**, 1250-1255.

450 **Kanie, T., Abbott, K. L., Mooney, N. A., Plowey, E. D., Demeter, J. and Jackson, P. K.** (2017). The  
451 CEP19-RABL2 GTPase Complex Binds IFT-B to Initiate Intraflagellar Transport at the Ciliary Base. *Dev Cell* **42**,  
452 22-36 e12.

453 **Kessler, K., Wunderlich, I., Uebe, S., Falk, N. S., Giessler, A., Brandstatter, J. H., Popp, B., Klinger, P.,  
454 Ekici, A. B., Sticht, H. et al.** (2015). DYNC2LI1 mutations broaden the clinical spectrum of dynein-2 defects.  
455 *Sci Rep* **5**, 11649.

456 **King, A., Hoch, N. C., McGregor, N. E., Sims, N. A., Smyth, I. M. and Heierhorst, J.** (2019). Dynll1 is  
457 essential for development and promotes endochondral bone formation by regulating intraflagellar Dynein  
458 function in primary cilia. *Hum Mol Genet.*

459 **King, S. M., Barbarese, E., Dillman, J. F., 3rd, Benashski, S. E., Do, K. T., Patel-King, R. S. and  
460 Pfister, K. K.** (1998). Cytoplasmic dynein contains a family of differentially expressed light chains.  
461 *Biochemistry* **37**, 15033-41.

462 **King, S. M. and Sale, W. S.** (2018). Fifty years of microtubule sliding in cilia. *Mol Biol Cell* **29**, 698-  
463 701.

464 **Kollmar, M.** (2016). Fine-Tuning Motile Cilia and Flagella: Evolution of the Dynein Motor Proteins  
465 from Plants to Humans at High Resolution. *Mol Biol Evol* **33**, 3249-3267.

466 **Kozminski, K. G., Johnson, K. A., Forscher, P. and Rosenbaum, J. L.** (1993). A motility in the  
467 eukaryotic flagellum unrelated to flagellar beating. *Proc Natl Acad Sci U S A* **90**, 5519-23.

468 **Li, C., Jensen, V. L., Park, K., Kennedy, J., Garcia-Gonzalo, F. R., Romani, M., De Mori, R., Bruel, A.  
469 L., Gaillard, D., Doray, B. et al.** (2016). MKS5 and CEP290 Dependent Assembly Pathway of the Ciliary  
470 Transition Zone. *PLoS Biol* **14**, e1002416.

471 **Li, W., Yi, P. and Ou, G.** (2015). Somatic CRISPR-Cas9-induced mutations reveal roles of  
472 embryonically essential dynein chains in *Caenorhabditis elegans* cilia. *J Cell Biol* **208**, 683-92.

473 **May, S. R., Ashique, A. M., Karlen, M., Wang, B., Shen, Y., Zarbalis, K., Reiter, J., Ericson, J. and**  
474 **Peterson, A. S.** (2005). Loss of the retrograde motor for IFT disrupts localization of Smo to cilia and  
475 prevents the expression of both activator and repressor functions of Gli. *Developmental Biology* **287**, 378-  
476 89.

477 **McInerney-Leo, A. M., Schmidts, M., Cortes, C. R., Leo, P. J., Gener, B., Courtney, A. D., Gardiner,**  
478 **B., Harris, J. A., Lu, Y., Marshall, M. et al.** (2013). Short-rib polydactyly and Jeune syndromes are caused by  
479 mutations in WDR60. *Am J Hum Genet* **93**, 515-23.

480 **Merrill, A. E., Merriman, B., Farrington-Rock, C., Camacho, N., Sebald, E. T., Funari, V. A., Schibler,**  
481 **M. J., Firestein, M. H., Cohn, Z. A., Priore, M. A. et al.** (2009). Ciliary abnormalities due to defects in the  
482 retrograde transport protein DYNC2H1 in short-rib polydactyly syndrome. *Am J Hum Genet* **84**, 542-9.

483 **Mijalkovic, J., Prevo, B., Oswald, F., Mangeol, P. and Peterman, E. J.** (2017). Ensemble and single-  
484 molecule dynamics of IFT dynein in *Caenorhabditis elegans* cilia. *Nat Commun* **8**, 14591.

485 **Mikami, A., Tynan, S. H., Hama, T., Luby-Phelps, K., Saito, T., Crandall, J. E., Besharse, J. C. and**  
486 **Vallee, R. B.** (2002). Molecular structure of cytoplasmic dynein 2 and its distribution in neuronal and  
487 ciliated cells. *Journal of Cell Science* **115**, 4801-8.

488 **Mirvis, M., Stearns, T. and James Nelson, W.** (2018). Cilium structure, assembly, and disassembly  
489 regulated by the cytoskeleton. *Biochem J* **475**, 2329-2353.

490 **Nachury, M. V. and Mick, D. U.** (2019). Establishing and regulating the composition of cilia for  
491 signal transduction. *Nat Rev Mol Cell Biol* **20**, 389-405.

492 **Orozco, J. T., Wedaman, K. P., Signor, D., Brown, H., Rose, L. and Scholey, J. M.** (1999). Movement  
493 of motor and cargo along cilia. *Nature* **398**, 674.

494 **Page, A. P.** (2018). The sensory amphidial structures of *Caenorhabditis elegans* are involved in  
495 macrocyclic lactone uptake and anthelmintic resistance. *Int J Parasitol* **48**, 1035-1042.

496 **Palmer, K. J., Hughes, H. and Stephens, D. J.** (2009). Specificity of cytoplasmic dynein subunits in  
497 discrete membrane-trafficking steps. *Molecular Biology of the Cell* **20**, 2885-99.

498 **Patel-King, R. S., Gilberti, R. M., Hom, E. F. and King, S. M.** (2013). WD60/FAP163 is a dynein  
499 intermediate chain required for retrograde intraflagellar transport in cilia. *Mol Biol Cell* **24**, 2668-77.

500 **Pazour, G. J., Baker, S. A., Deane, J. A., Cole, D. G., Dickert, B. L., Rosenbaum, J. L., Witman, G. B.**  
501 **and Besharse, J. C.** (2002). The intraflagellar transport protein, IFT88, is essential for vertebrate  
502 photoreceptor assembly and maintenance. *J Cell Biol* **157**, 103-13.

503 **Pazour, G. J., Dickert, B. L., Vucica, Y., Seeley, E. S., Rosenbaum, J. L., Witman, G. B. and Cole, D.**  
504 **G.** (2000). Chlamydomonas IFT88 and its mouse homologue, polycystic kidney disease gene tg737, are  
505 required for assembly of cilia and flagella. *J Cell Biol* **151**, 709-18.

506 **Pazour, G. J., Dickert, B. L. and Witman, G. B.** (1999a). The DHC1b (DHC2) isoform of cytoplasmic  
507 dynein is required for flagellar assembly. *J Cell Biol* **144**, 473-81.

508 **Pazour, G. J., Koutoulis, A., Benashski, S. E., Dickert, B. L., Sheng, H., Patel-King, R. S., King, S. M.**  
509 **and Witman, G. B.** (1999b). LC2, the chlamydomonas homologue of the t complex-encoded protein Tctex2,  
510 is essential for outer dynein arm assembly. *Molecular Biology of the Cell* **10**, 3507-20.

511 **Pazour, G. J., Wilkerson, C. G. and Witman, G. B.** (1998). A dynein light chain is essential for the  
512 retrograde particle movement of intraflagellar transport (IFT). *J Cell Biol* **141**, 979-92.

513 **Pedersen, L. B., Miller, M. S., Geimer, S., Leitch, J. M., Rosenbaum, J. L. and Cole, D. G.** (2005).  
514 Chlamydomonas IFT172 is encoded by FLA11, interacts with CrEB1, and regulates IFT at the flagellar tip.  
515 *Curr Biol* **15**, 262-6.

516 **Porter, M. E., Bower, R., Knott, J. A., Byrd, P. and Dentler, W.** (1999). Cytoplasmic dynein heavy  
517 chain 1b is required for flagellar assembly in Chlamydomonas. *Mol Biol Cell* **10**, 693-712.

518 **Raaijmakers, J. A. and Medema, R. H.** (2014). Function and regulation of dynein in mitotic  
519 chromosome segregation. *Chromosoma* **123**, 407-22.

520 **Reck-Peterson, S. L., Redwine, W. B., Vale, R. D. and Carter, A. P.** (2018). The cytoplasmic dynein  
521 transport machinery and its many cargoes. *Nat Rev Mol Cell Biol* **19**, 382-398.



522 **Reck, J., Schauer, A. M., VanderWaal Mills, K., Bower, R., Tritschler, D., Perrone, C. A. and Porter,**  
523 **M. E.** (2016). The role of the dynein light intermediate chain in retrograde IFT and flagellar function in  
524 Chlamydomonas. *Mol Biol Cell* **27**, 2404-22.

525 **Reiter, J. F. and Leroux, M. R.** (2017). Genes and molecular pathways underpinning ciliopathies.  
526 *Nat Rev Mol Cell Biol* **18**, 533-547.

527 **Roberts, A. J.** (2018). Emerging mechanisms of dynein transport in the cytoplasm versus the cilium.  
528 *Biochem Soc Trans* **46**, 967-982.

529 **Rompolas, P., Pedersen, L. B., Patel-King, R. S. and King, S. M.** (2007). Chlamydomonas FAP133 is a  
530 dynein intermediate chain associated with the retrograde intraflagellar transport motor. *Journal of Cell*  
531 *Science* **120**, 3653-65.

532 **Rosenbaum, J. L. and Witman, G. B.** (2002). Intraflagellar transport. *Nat Rev Mol Cell Biol* **3**, 813-25.

533 **Scheidel, N. and Blacque, O. E.** (2018). Intraflagellar Transport Complex A Genes Differentially  
534 Regulate Cilium Formation and Transition Zone Gating. *Curr Biol* **28**, 3279-3287 e2.

535 **Schmidt, H., Zalyte, R., Urnavicius, L. and Carter, A. P.** (2015). Structure of human cytoplasmic  
536 dynein-2 primed for its power stroke. *Nature* **518**, 435-438.

537 **Schmidts, M., Arts, H. H., Bongers, E. M., Yap, Z., Oud, M. M., Antony, D., Duijkers, L., Emes, R. D.,**  
538 **Stalker, J., Yntema, J. B. et al.** (2013a). Exome sequencing identifies DYNC2H1 mutations as a common  
539 cause of asphyxiating thoracic dystrophy (Jeune syndrome) without major polydactyly, renal or retinal  
540 involvement. *Journal of Medical Genetics* **50**, 309-23.

541 **Schmidts, M., Hou, Y., Cortes, C. R., Mans, D. A., Huber, C., Boldt, K., Patel, M., van Reeuwijk, J.,**  
542 **Plaza, J. M., van Beersum, S. E. et al.** (2015). TCTEX1D2 mutations underlie Jeune asphyxiating thoracic  
543 dystrophy with impaired retrograde intraflagellar transport. *Nat Commun* **6**, 7074.

544 **Schmidts, M. and Mitchison, H. M.** (2018). 15 - Severe skeletal abnormalities caused by defects in  
545 retrograde intraflagellar transport dyneins. In *Dyneins (Second Edition)*, (ed. S. M. King), pp. 356-401:  
546 Academic Press.

547 **Schmidts, M., Vodopituz, J., Christou-Savina, S., Cortes, C. R., McInerney-Leo, A. M., Emes, R. D.,**  
548 **Arts, H. H., Tuysuz, B., D'Silva, J., Leo, P. J. et al.** (2013b). Mutations in the gene encoding IFT dynein  
549 complex component WDR34 cause Jeune asphyxiating thoracic dystrophy. *Am J Hum Genet* **93**, 932-44.

550 **Schouteden, C., Serwas, D., Palfy, M. and Dammermann, A.** (2015). The ciliary transition zone  
551 functions in cell adhesion but is dispensable for axoneme assembly in *C. elegans*. *J Cell Biol* **210**, 35-44.

552 **Schroeder, C. M., Ostrem, J. M., Hertz, N. T. and Vale, R. D.** (2014). A Ras-like domain in the light  
553 intermediate chain bridges the dynein motor to a cargo-binding region. *Elife* **3**, e03351.

554 **Signor, D., Wedaman, K. P., Orozco, J. T., Dwyer, N. D., Bargmann, C. I., Rose, L. S. and Scholey, J.**  
555 **M.** (1999). Role of a class DHC1b dynein in retrograde transport of IFT motors and IFT raft particles along  
556 cilia, but not dendrites, in chemosensory neurons of living *Caenorhabditis elegans*. *J Cell Biol* **147**, 519-30.

557 **Stepanek, L. and Pigino, G.** (2016). Microtubule doublets are double-track railways for intraflagellar  
558 transport trains. *Science* **352**, 721-4.

559 **Sun, S., Fisher, R. L., Bowser, S. S., Pentecost, B. T. and Sui, H.** (2019). Three-dimensional  
560 architecture of epithelial primary cilia. *Proc Natl Acad Sci U S A* **116**, 9370-9379.

561 **Tanaka, Y., Zhang, Z. and Hirokawa, N.** (1995). Identification and molecular evolution of new  
562 dynein-like protein sequences in rat brain. *Journal of Cell Science* **108 ( Pt 5)**, 1883-93.

563 **Taschner, M. and Lorentzen, E.** (2016). The Intraflagellar Transport Machinery. *Cold Spring Harb*  
564 *Perspect Biol* **8**.

565 **Taylor, S. P., Dantas, T. J., Duran, I., Wu, S., Lachman, R. S., University of Washington Center for**  
566 **Mendelian Genomics, C., Nelson, S. F., Cohn, D. H., Vallee, R. B. and Krakow, D.** (2015). Mutations in  
567 DYNC2LI1 disrupt cilia function and cause short rib polydactyly syndrome. *Nat Commun* **6**, 7092.

568 **Toropova, K., Mladenov, M. and Roberts, A. J.** (2017). Intraflagellar transport dynein is  
569 autoinhibited by trapping of its mechanical and track-binding elements. *Nat Struct Mol Biol* **24**, 461-468.

570 **Toropova, K., Zalyte, R., Mukhopadhyay, A. G., Mladenov, M., Carter, A. P. and Roberts, A. J.**  
571 (2019). Structure of the dynein-2 complex and its assembly with intraflagellar transport trains. *Nat Struct*  
572 *Mol Biol* **26**, 823-829.

573 **Tsao, C. C. and Gorovsky, M. A.** (2008). Different effects of Tetrahymena IFT172 domains on  
574 anterograde and retrograde intraflagellar transport. *Mol Biol Cell* **19**, 1450-61.

575 **Tsurumi, Y., Hamada, Y., Katoh, Y. and Nakayama, K.** (2019). Interactions of the dynein-2  
576 intermediate chain WDR34 with the light chains are required for ciliary retrograde protein trafficking. *Mol*  
577 *Biol Cell* **30**, 658-670.

578 **Vuolo, L., Stevenson, N. L., Heesom, K. J. and Stephens, D. J.** (2018). Dynein-2 intermediate chains  
579 play crucial but distinct roles in primary cilia formation and function. *Elife* **7**.

580 **Wang, W. J., Tay, H. G., Soni, R., Perumal, G. S., Goll, M. G., Macaluso, F. P., Asara, J. M., Amack,**  
581 **J. D. and Tsou, M. F.** (2013). CEP162 is an axoneme-recognition protein promoting ciliary transition zone  
582 assembly at the cilia base. *Nat Cell Biol* **15**, 591-601.

583 **Wei, Q., Zhang, Y., Li, Y., Zhang, Q., Ling, K. and Hu, J.** (2012). The BBSome controls IFT assembly  
584 and turnaround in cilia. *Nat Cell Biol* **14**, 950-7.

585 **Wicks, S. R., de Vries, C. J., van Luenen, H. G. and Plasterk, R. H.** (2000). CHE-3, a cytosolic dynein  
586 heavy chain, is required for sensory cilia structure and function in *Caenorhabditis elegans*. *Developmental*  
587 *Biology* **221**, 295-307.

588 **Wickstead, B. and Gull, K.** (2007). Dyneins across eukaryotes: a comparative genomic analysis.  
589 *Traffic* **8**, 1708-21.

590 **Wiegner, A., Dildrop, R., Kalfhues, L., Spychala, A., Kuschel, S., Lier, J. M., Zobel, T., Dahmen, S.,**  
591 **Leu, T., Struchtrup, A. et al.** (2018). Cell type-specific regulation of ciliary transition zone assembly in  
592 vertebrates. *EMBO J* **37**.

593 **Williams, C. L., McIntyre, J. C., Norris, S. R., Jenkins, P. M., Zhang, L., Pei, Q., Verhey, K. and**  
594 **Martens, J. R.** (2014). Direct evidence for BBSome-associated intraflagellar transport reveals distinct  
595 properties of native mammalian cilia. *Nat Commun* **5**, 5813.

596 **Williamson, S. M., Silva, D. A., Richey, E. and Qin, H.** (2012). Probing the role of IFT particle  
597 complex A and B in flagellar entry and exit of IFT-dynein in *Chlamydomonas*. *Protoplasma* **249**, 851-6.

598 **Wingfield, J. L., Mengoni, I., Bomberger, H., Jiang, Y. Y., Walsh, J. D., Brown, J. M., Picariello, T.,**  
599 **Cochran, D. A., Zhu, B., Pan, J. et al.** (2017). IFT trains in different stages of assembly queue at the ciliary  
600 base for consecutive release into the cilium. *Elife* **6**.

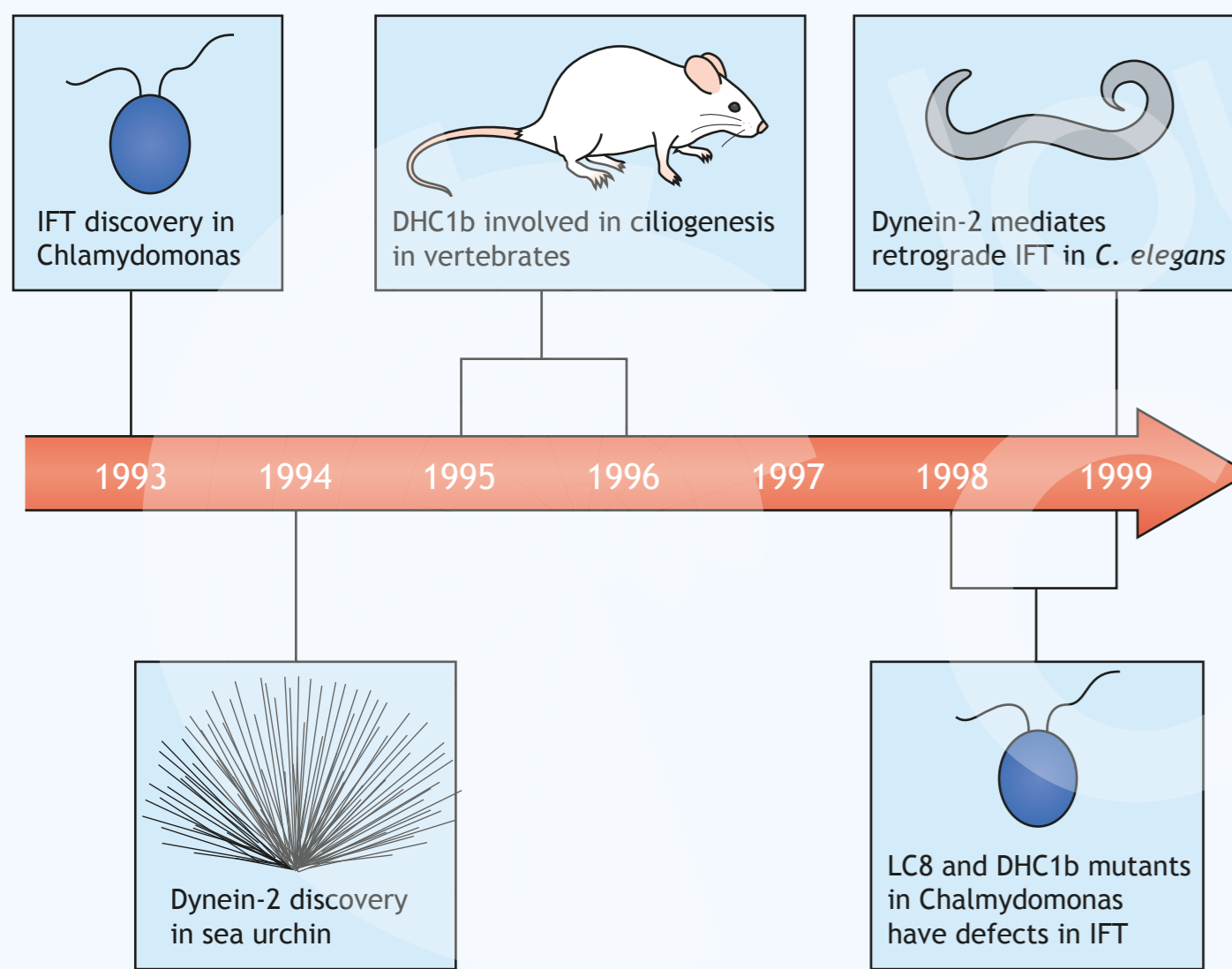
601 **Wu, C., Li, J., Peterson, A., Tao, K. and Wang, B.** (2017). Loss of dynein-2 intermediate chain Wdr34  
602 results in defects in retrograde ciliary protein trafficking and Hedgehog signaling in the mouse. *Hum Mol*  
603 *Genet* **26**, 2386-2397.

604 **Yang, T. T., Su, J., Wang, W. J., Craige, B., Witman, G. B., Tsou, M. F. and Liao, J. C.** (2015).  
605 Superresolution Pattern Recognition Reveals the Architectural Map of the Ciliary Transition Zone. *Sci Rep* **5**,  
606 14096.

607

608

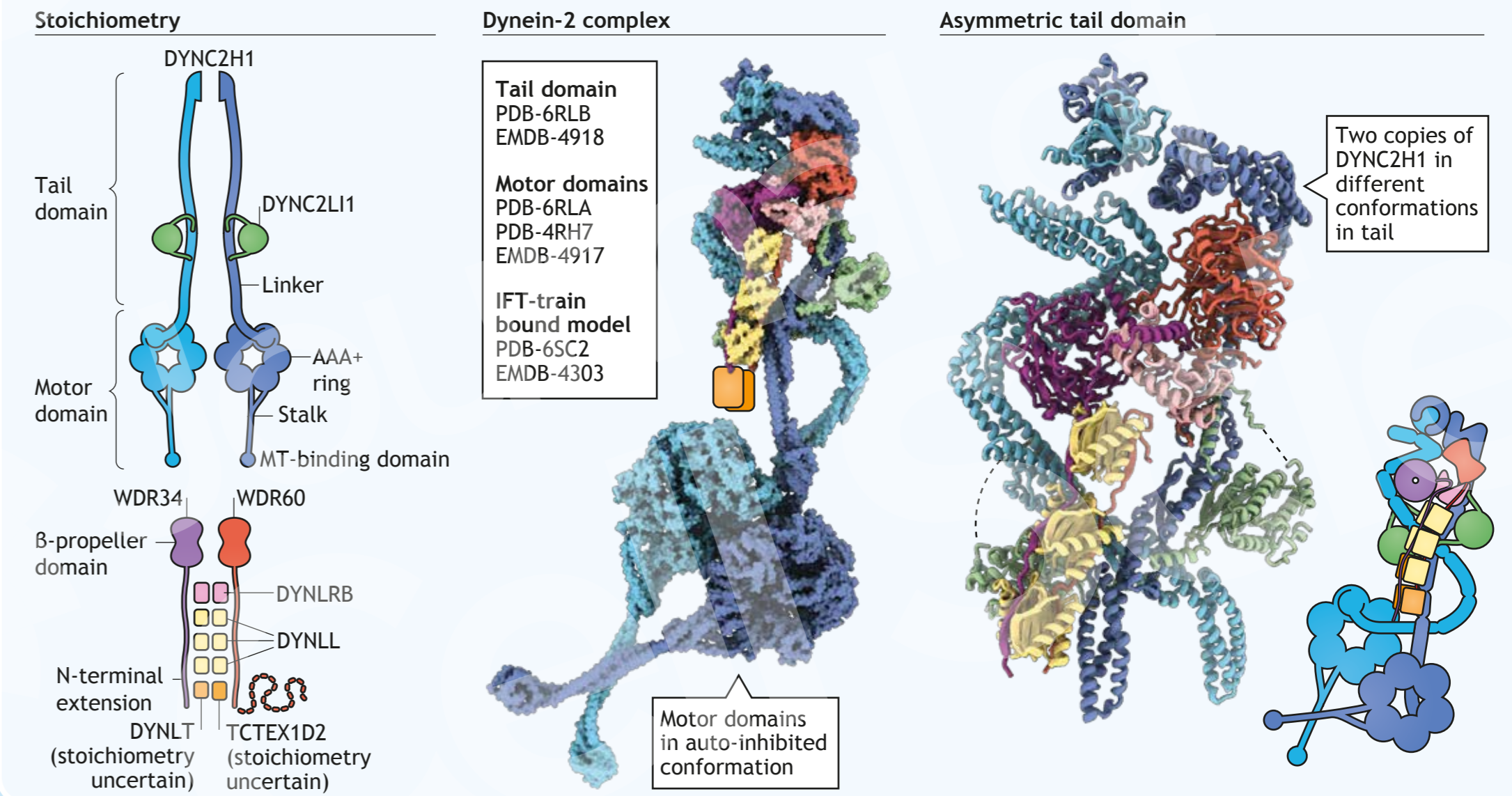
## Discovery of dynein-2 and its involvement in IFT



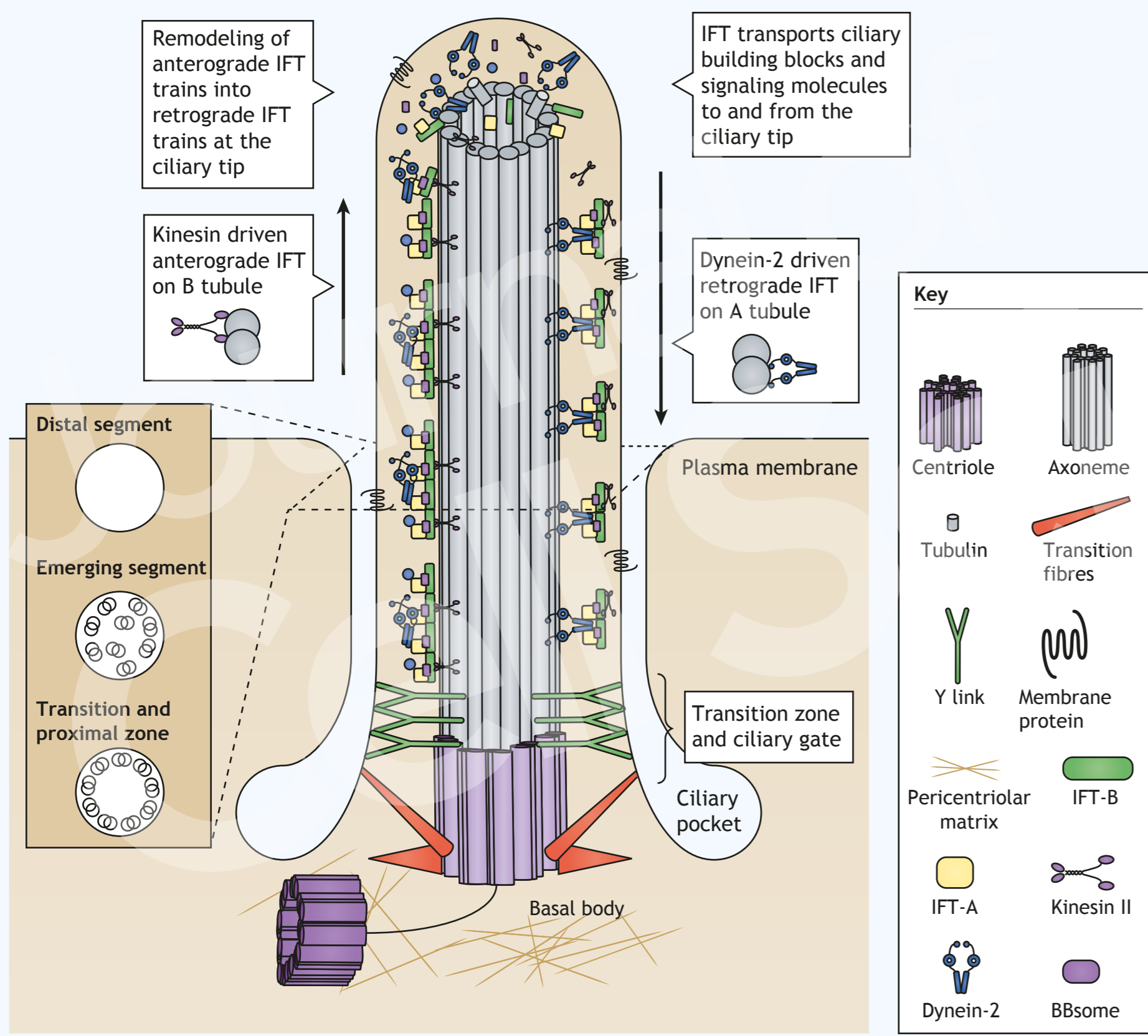
## Subunit composition of dynein-2

Chain type	Alias	<i>H. sapiens</i>	<i>C. reinhardtii</i>	<i>C. elegans</i>	Structure	Size (amino acids)	
Heavy	DHC2	DYNC2H1	DHC1b	CHE-3	Tail, Motor domain	4,307 ( <i>H. sapiens</i> )	
	Intermediate	WDR60	D1bIC1 (FAP163)	Ambiguous	β-propeller domain	1066	
Intermediate	WDR34	WDR34	D1bIC2 (FAP133)	Ambiguous	β-propeller domain	536	
	Light intermediate	LIC3	DYNC2L11	D1bLIC	XBX-1	Ras-like domain	351
Light	RB	DYNLRB1 DYNLRB2	LC7b LC7a	DYRB-1	1	96	Also found in cytoplasmic dynein-1
	LC8	DYNLL1 DYNLL2	LC8	DLC-1	1	89	Also found in cytoplasmic dynein-1
Light	TCTEX	DYNLT1 DYNLT3	Tctex1	DYLT-1 DYLT-3	1	113	Also found in cytoplasmic dynein-1
	TCTEX1D2	TCTEX1D2	Tctex2b	DYLT-2	1	142	

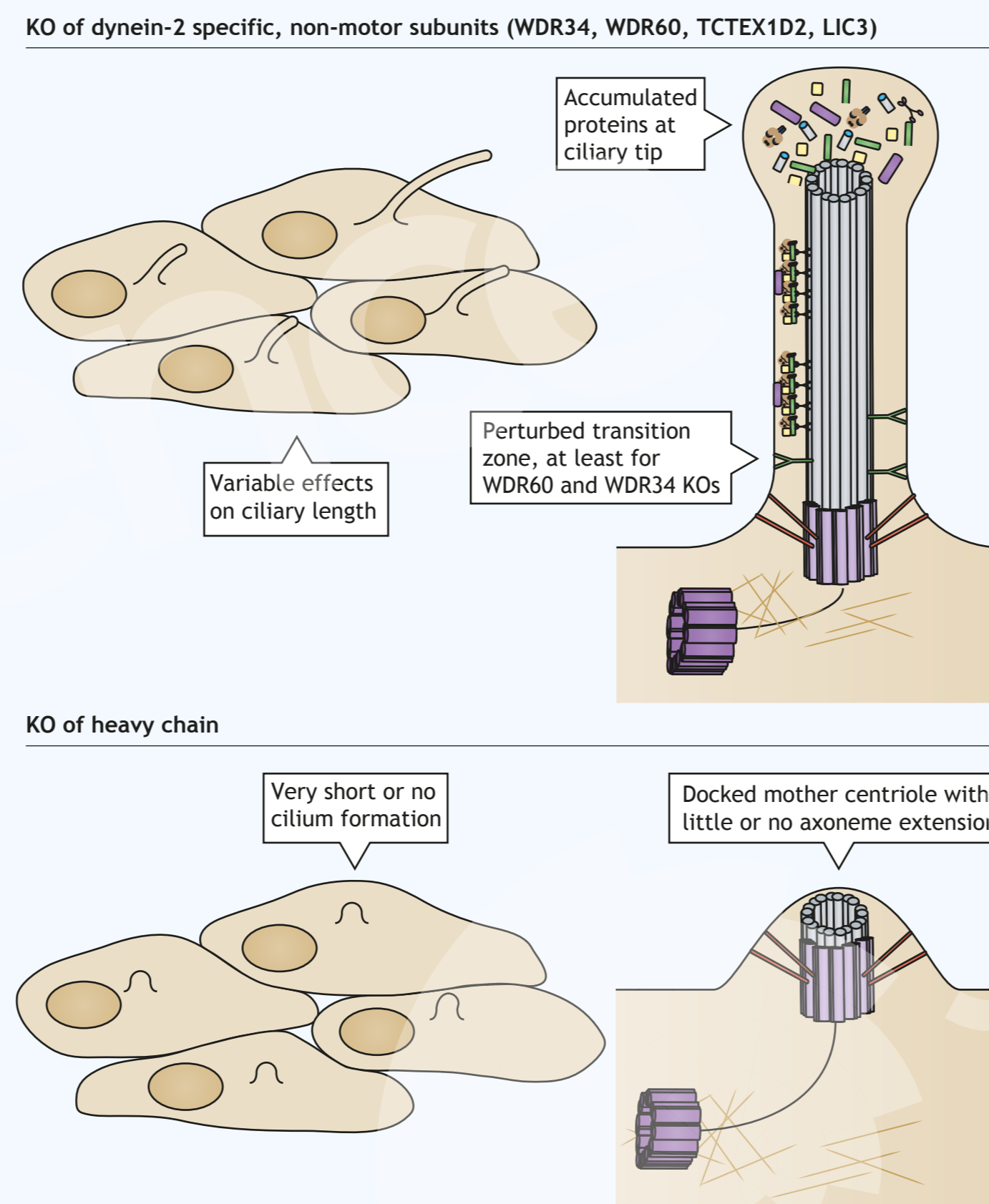
## Structure of dynein-2



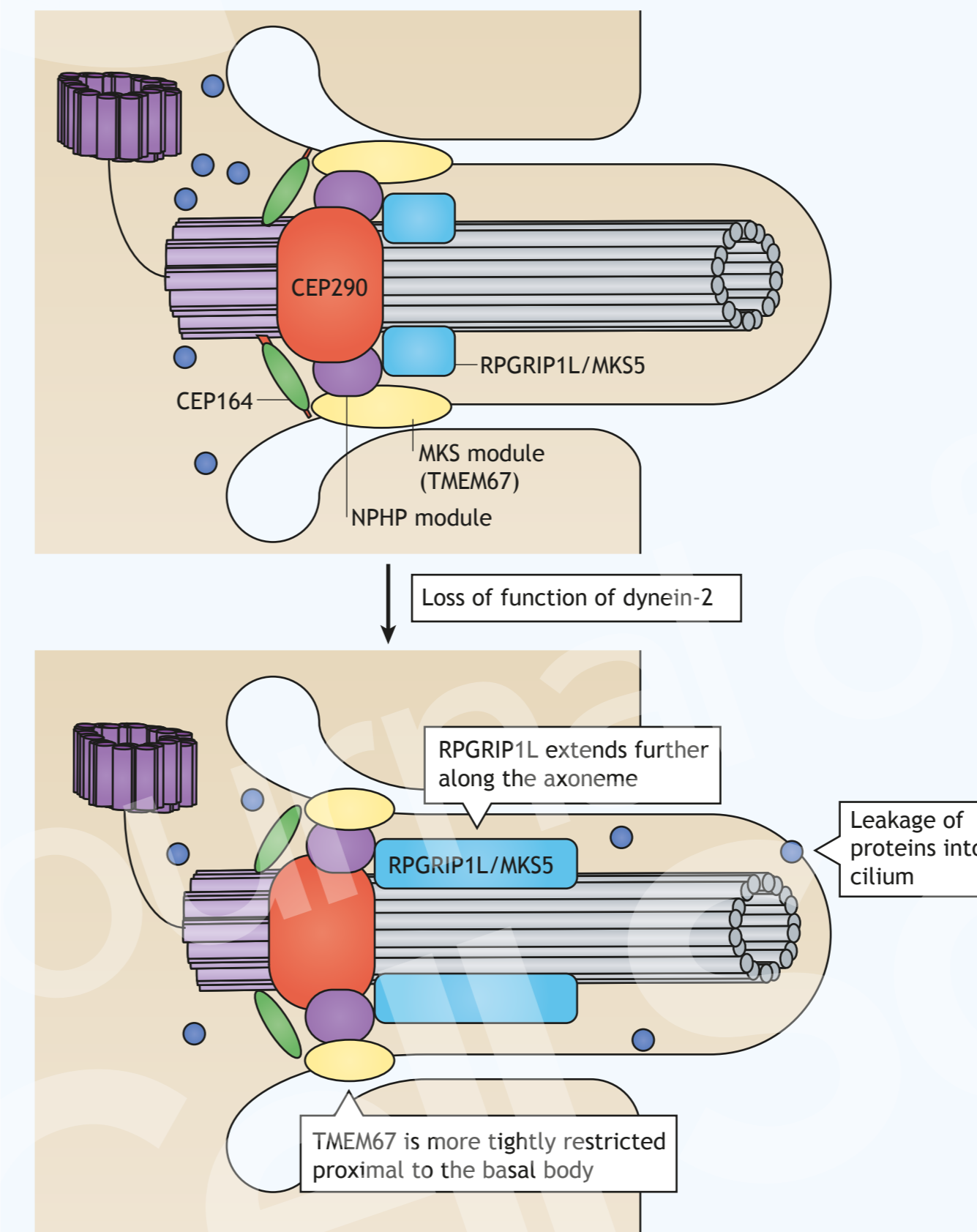
## Role of dynein-2 in the bidirectional IFT system



## Impact of dynein-2 subunit mutants



## Dynein-2 and the ciliary transition zone



## Dynein-2 activation at ciliary tip

